Supplementary Information: A Review and Experimental Revisit of Alternative Catalysts for Selective Oxidation of Methanol to Formaldehyde

Joachim Thrane [1], Uffe Vie Mentzel [2], Max Thorhauge [2], Martin Høj [1] and Anker Degn Jensen [1,*]

[1] Department of Chemical and Biochemical Engineering, Technical University of Denmark (DTU), DK-2800 Kgs. Lyngby, Denmark.
[2] Haldor Topsøe A/S, DK-2800 Kgs. Lyngby, Denmark.
* Correspondence: aj@kt.dtu.dk

Contents

1. Experimental

1.1. Catalyst Synthesis

Table S1. Overview of catalyst systems which were revisited.

#	Type	Preparation Method	Aim
1	Fe_2O_3/MgO	Incipient wetness impregnation	8.2 wt% Fe_2O_3
2	Fe_2O_3/MgO	Incipient wetness impregnation	15.2 wt% Fe_2O_3
3	V_2O_5/HAP	Incipient wetness impregnation	3.0 wt% V_2O_5
4	V_2O_5/HAP	Incipient wetness impregnation	5 wt% V_2O_5
5	Nb_2O_5/HAP	Incipient wetness impregnation	2.6 wt% Nb_2O_5
6	Nb_2O_5/HAP	Incipient wetness impregnation	5 wt% Nb_2O_5
7	MoO_3/α-Al_2O_3	Incipient wetness impregnation	6.2 wt% MoO_3
8	MoO_3/α-Al_2O_3	Incipient wetness impregnation	1 wt% MoO_3
9	V_2O_5/α-Al_2O_3	Incipient wetness impregnation	1 wt% V_2O_5
10	Nb_2O_5/α-Al_2O_3	Incipient wetness impregnation	0.5 wt% Nb_2O_5
11	Nb_2O_5/α-Al_2O_3	Incipient wetness impregnation	1 wt% Nb_2O_5
12	MoO_3/MgO	Incipient wetness impregnation	10 wt% MoO_3
13	SbO/SiO_2	Incipient wetness impregnation	20 wt% Sb_2O_5
14	Nb_2O_5	Reflux	Aimed for NbPO
15a	VPO	Reflux	V/P = 1/1 mol/mol
15b	VPO	Reflux	V/P = 1/1 mol/mol
16	$FeVO_4$	Citric acid network	Fe/V = 1/1 mol/mol
17	$FeVO_4$-Cl	Incipient wetness impregnation	1 wt% Cl on sample #16
18	V-Sb-O	Co-precipitation	10 wt% V_2O_5
19	Mo-Sb-O	Co-precipitation	10 wt% MoO_3
20	NbPO	Co-precipitation	Nb/P = 1/1 mol/mol

1.1.1. Chemicals Used for Synthesis

$Mg(OH)_2$ (Sigma-Aldrich; BioUltra, ≥ 99.0% (KT)), $Fe(NO_3)_3 \cdot 9H_2O$ (Sigma-Aldrich; ACS reagent, ≥98%), Deionized water, hydroxyapatite (HAP) (Sigma-Aldrich, purum p.a., ≥90% (as $Ca_3(PO_4)_2$,KT)), $(NH_4)_6Mo_7O_{24} \cdot 4H_2O$ (Sigma-Aldrich; puriss. p.a., ACS reagent, ≥99.0% (T)), NH_4VO_3 (Sigma-Aldrich; ACS reagent, ≥99.0%), $C_6H_8O_8 \cdot H_2O$ (Sigma-Aldrich; ACS Reagent,

≥99.0%), $NH_4NbO(C_2O_4)_2$ (Sigma-Aldrich, 99.99% trace metal basis), antimony(III) acetate (Sigma-Aldrich, 99.99% trace metals basis), Nb_2O_5 (Sigma-Aldrich; 99.9% trace metal basis), 85 wt% ortho-H_3PO_4 (Fluka, purum p.a. ≥ 85% (T)), V_2O_5 (Sigma-Aldrich; ≥98%), NH_4Cl (Fluka, BioUltra, for molecular biologym ≥99.5% (AT)), $SbCl_5$ (Sigma-Aldrich, 99%), urea, $(NH_4)_2HPO_4$ (Sigma-Aldrich; BioUltra, ≥99.0% (T)).

1.1.2. Impregnated Catalysts

Fe_2O_3/MgO

5 g of 8.2 wt% Fe_2O_3/MgO and 15.2 wt% Fe_2O_3/MgO were prepared by incipient wetness impregnation. The pore volume of $Mg(OH)_2$ (Sigma-Aldrich; BioUltra, ≥ 99.0% (KT)) was found to be app. 1.1 g H_2O/g $Mg(OH)_2$. 1.9585 g and 3.9207 g of $Fe(NO_3)_3 \cdot 9H_2O$ (Sigma-Aldrich; ACS reagent, ≥98%) were dissolved in 6.7 g and 6.1 g of H_2O, which were added to 6.132 g and 6.136 of $Mg(OH)_2$ respectively. The samples were dried at 50°C. The 8.2 wt% Fe_2O_3/MgO sample was calcined in a tubular oven with a ramping rate of 5°C/min to 500°C. The temperature was held for 4 h. During calcination there was an air flow of 607 NmL/min. For the 15.2 wt% Fe_2O_3/MgO sample calcination was done in static air utilizing a muffle furnace. The samples were pressed, crushed and sieved to 150-250 μm.

V_2O_5/HAP and Nb_2O_5/HAP

The pore volume of hydroxyapatite from Sigma-Aldrich (HAP) (Sigma-Aldrich, purum p.a., ≥90% (as $Ca_3(PO_4)_2$)) was determined to be app. 1.9 g H_2O/g HAP.

4 g of samples with two different loadings of V_2O_5 or Nb_2O_5 impregnated on HAP were prepared. The respective amounts of NH_4VO_3 and $C_6H_8O_8 \cdot H_2O$ to help dissolve the NH_4VO_3, or $NH_4NbO(C_2O_4)_2$ were dissolved in the corresponding amount of H_2O (Table S2). This was added to HAP powder, mixed and dried at 50°C. V_2O_5 samples were re-wetted with H_2O and dried once more at 50°C as the samples looked to be different in color from the top to the bottom. The samples were calcined with a ramping rate of 4°C/min to 400°C for 4 h. Calcination was performed in static air in a muffle furnace. The samples were pressed, crushed and sieved to 150-250 μm.

Table S2. Amounts of chemicals used for the preparation of HAP supported samples.

Loading	**HAP**	**$C_6H_8O_8 \cdot H_2O$**	**NH_4VO_3**	**$NH_4NbO(C_2O_4)_2$**
	[g]	**[g]**	**[g]**	**[g]**
3 wt% V_2O_5	3.800	0.342	0.155	-
5 wt% V_2O_5	3.801	0.592	0.257	-
2.6 wt% Nb_2O_5	3.804	-	-	0.228
5 wt% Nb_2O_5	3.808	-	-	0.459

MoO_3/α-Al_2O_3, V_2O_5/α-Al_2O_3, Nb_2O_5/α-Al_2O_3

α-Al_2O_3 pellets from Haldor Topsøe A/S were crushed and sieved to 150-250 μm. The pore volume was then determined to be 1 g H_2O/g α-Al_2O_3.

4 g of samples with different loadings of MoO_3, V_2O_5 or Nb_2O_5 impregnated on α-Al_2O_3 were prepared by impregnation. The respective amounts of $(NH_4)_6Mo_7O_{24}{\cdot}4H_2O$, NH_4VO_3 and $C_6H_8O_8{\cdot}H_2O$ to help dissolve the NH_4VO_3, or $NH_4NbO(C_2O_4)_2$ were dissolved in the corresponding amount of water (Table S3), added to the α-Al_2O_3 and mixed. The samples were dried at 50°C. The samples were calcined with a ramping rate of 5°C/min to 500°C (MoO_3) and 400°C (V_2O_5, Nb_2O_5), which were held for 4 h. The calcination was in static air in a muffle furnace.

Table S3. Amounts of chemicals used for the preparation of α-Al_2O_3 supported samples.

Loading	**α-Al_2O_3**	**$(NH_4)_6Mo_7O_{24}{\cdot}4H_2O$**	**$C_6H_8O_8{\cdot}H_2O$**	**NH_4VO_3**	**$NH_4NbO(C_2O_4)_2$**
	[g]	**[g]**	**[g]**	**[g]**	**[g]**
6.2 wt% MoO_3	3.9624	0.326	-	-	-
1 wt% MoO_3	3.9601	0.047	-	-	-
1 wt% V_2O_5	3.9629	-	0.122	0.052	-
0.5 wt% Nb_2O_5	3.9734	-	-	-	0.046
1 wt% Nb_2O_5	3.9603	-	-	-	0.092

MoO_3/MgO

4 g of 10 wt% MoO_3/MgO was prepared by impregnation. 0.465 g of $(NH_4)_6Mo_7O_{24}{\cdot}4H_2O$ was dissolved in 5.35 g of H_2O, which was added to 5.211 g of $Mg(OH)_2$ and mixed. The sample was dried at 60°C. Calcination was done in static air in a muffle furnace with a ramping rate of 5°C/min to 500°C, which was held for 4 h.

SbO/SiO_2

4 g of antimony oxide (aim: 20 wt% Sb_2O_5) on SiO_2 was prepared by incipient wetness impregnation. The loading of antimony was chosen to obtain monolayer coverage. The pore volume of the SiO_2 was found to be 2.36 g H_2O/g SiO_2. For the impregnation, 1.476 g of antimony(III) acetate was dissolved in 7.56 g of glacial acetic acid (some solid antimony oxide formed due to water impurities in the solvent). This was added to 3.2068 g of crushed and sieved (150-250 μm) SiO_2 pellets (Chempur, 250 m^2/g) and mixed. The sample was dried at 60°C and calcined in static air in a muffle furnace with a heating rate of 5°C/min to 500°C, which was held for 4 h.

1.1.3. Refluxed Catalysts

$NbOPO_4$

It was aimed to synthesize 5 g of NbPO, however, as will be shown in Section 2.1.1 in the SI, this was not accomplished. 3.532 g of Nb_2O_5 was added to 100 mL of H_2O together with 29.897 g of 85

wt% ortho-H_3PO_4 in a round bottomed flask. The mixture was refluxed for 24 h under stirring, cooled and filtered, washed with 500 mL of H_2O and dried at 40°C over night, resulting in a fluffy powder.

Vanadium Phosphates

10 g of vanadium phosphate was prepared following the procedure of Behera et al. [1,2]. 4.870 g of V_2O_5 and 55.026 g of 85 wt% H_3PO_4 was added to 150 mL of H_2O in a round bottomed flask and was refluxed under stirring for 24 h, vacuum filtered, and washed with 500 mL of H_2O. The filter cake and filtrate were yellow.

The sample was dried at 50°C for 4 days and over night at 110°C (giving $VOPO_4 \cdot 2H_2O$ [1,2]). 2.3178 g of the synthesized $VOPO_4 \cdot 2H_2O$ (app. half of the yielded solid) was mixed with 80 mL of isobutanol and refluxed under stirring for 21 h. The solid changed color from yellow to green/blue. The solid was filtered and washed with 600 mL of H_2O and was dried at 100°C (giving VPO (15a) precursor $VOHPO_4 \cdot 0.5H_2O$ [1], [2]). 1.9393 g was added to 38 mL of H_2O and refluxed for 2 h as in [1,2]. The mixture was filtered hot. Both filter cake and filtrate were bluish. The filter cake was dried at 50°C, giving sample VPO (15b) precursor. Both VPO (15a) and VPO (15b) were calcined at 400°C for 4 h in static air in a muffle furnace with a ramping rate of 5°C/min in static air in a muffle furnace. The yield after calcination was app. 2.1 g of VPO (15a) and 1 g of VPO (15b), thus much was lost during the preparation.

1.1.4. Iron Vanadate

5 g of $FeVO_4$ was synthesized by a method inspired by Liu et al. [3]. 11.8257 g of $Fe(NO_3)_3 \cdot 9H_2O$, 3.4247 g of NH_4VO_3 and 8.0985 g of citric acid monohydrate were mixed with 100 mL of H_2O in a round bottomed flask and stirred rigorously for 1 h. The water was removed at 80°C in a vacuum rotary evaporator. The sample was dried at 110°C over night and calcined with a heating ramp of 5°C/min to 400°C, held for 6 h in static air.

A sample was further doped with Cl to test an idea of poisoning basic sites (in the same way as alkali metals poison acidic sites) and thus decrease the tendency of over-oxidation to CO and CO_2. This was done with 0.4930 g of the prepared $FeVO_4$ catalyst as sieve fraction 150-250 μm. It was impregnated with 0.0087 g of NH_4Cl, which was first dissolved in 0.65 g of water, then added to the $FeVO_4$, with additional 0.53 g of water and mixed before drying at 60°C. The sample was calcined with a ramp of 5°C/min to 400°C, held for 4 h.

1.1.5. Co-Precipitated Catalysts

V-Sb-O and Mo-Sb-O

5 g of V-Sb mixed metal oxide catalyst was prepared by co-precipitation inspired from [4,5]. 0.646 g of NH_4VO_3 was dissolved in 300 mL of H_2O with the addition of 1.563 g of citric acid monohydrate to help dissolving the NH_4VO_3. This happened over night. The solution was first yellow but became blue during the night.

40.037 g of urea was dissolved in 400 mL of H_2O. 3.74 mL of $SbCl_5$ was added to the urea solution under stirring over 30 min using a KD Scientific syringe pump model 100. As $SbCl_5$ is sensitive to water vapor, care was taken to minimize air exposure, and care should be taken to avoid exposure to HCl formed. In the same period the 300 mL metavanadate solution was added uniformly by use of a conical separation funnel. The solution was aged for 30 min, after which 50 mL of 25 wt% ammonia solution was added, pH became app. 10.5, and the solution became more white than yellowish. The mixture was filtered and the filter cake was washed with 2 x 500 mL of H_2O. The sample was dried at 100°C and calcined at 500°C for 4 h with a heating rate of 5°C/min in static air in a muffle furnace.

5 g of 10 Mo-Sb mixed metal oxide catalyst was similarly prepared by co-precipitation. 0.6133 g of $(NH_4)_6Mo_7O_{24}{\cdot}4H_2O$ was dissolved in 300 mL of H_2O. 40.36 g of urea was dissolve in 400 mL of H_2O. The same amount of $SbCl_5$ and procedure as for the V_2O_5/Sb_2O_4 sample was followed. The precipitated solids were more difficult to retain, and the yield of catalyst after calcination was only app. 0.35 g.

NbPO

5 g of niobium phosphate was prepared by drying precipitation. 7.4315 g of $NH_4NbO(C_2O_4)_2{\cdot}xH_2O$ was dissolved in 49.45 g of H_2O by stirring. 3.2320 g of $(NH_4)_2HPO_4$ was dissolved in 29.71 g of H_2O. The phosphate solution was poured into the niobate solution under stirring. No precipitation was observed. The solution was put to drying at 75°C, calcined at 400°C for 4 h in static air, heating rate of 5°C/min.

1.2. Catalyst Characterization

X-ray powder diffraction, ICP-OES, and BET were performed as described previously in [6].

1.3. Catalytic Activity and Selectivity

Catalytic activity, selectivity and stability were measured using a lab scale, fixed bed reactor setup described in detail elsewhere [7–9]. The measurements were mostly carried out using 50 mg of catalyst in a 150-250 μm sieve fraction diluted with 150 mg of SiC (150-355 μm) in a feed of 127.5 NmL/min N_2, 15 NmL/min O_2 and 3-5 vol.% MeOH. The activity tests, data acquisition and data

treatment were conducted as described previously [6]. The FID detector in the GC was unavailable during the measurement campaign, thus methyl formate and dimethoxymethane were not measured.

Conversion and selectivity were calculated according to Equations (S1) and (S2).

$$S_i = \frac{v_i y_i}{\sum_i v_i y_i} \tag{S1}$$

$$X = \frac{\sum_i v_i y_i}{y_{CH_3OH} + \sum_i v_i y_i} \tag{S2}$$

Where S_i was the selectivity towards the i'th product, v_i was the number of carbon atoms in the i'th specie (not including methanol), y_i was the measured mole fraction of the i'th species and X was the conversion. The DME corrected selectivity (S_{cor}) was often used as the selectivity towards formaldehyde, as DME is a reversible byproduct consisting of two methanol. The DME corrected selectivity to FA was calculated according to Equation (S3).

$$S_{cor} = \frac{S_{\mathrm{CH_2O}}}{S_{\mathrm{CH_2O}} + S_{\mathrm{CO}} + S_{\mathrm{CO_2}}} \tag{S3}$$

Furthermore, also the DME corrected conversion was used and was calculated according to Equation (S4).

$$X_{cor} = (1 - S_{\mathrm{DME}})X \tag{S4}$$

The rate constants were calculated under assumption of first order kinetics w.r.t. methanol [10,11] from the design equation for a first order reaction in a PFR reactor, as shown in Equation (S5)

$$k = \frac{V_0}{W_{cat}} \ln(1 - X) \tag{S5}$$

Where V_0 was the actual volumetric flowrate at reaction temperature and pressure in the reactor. The activation energy (E_a) could be found by linear regression on the modified Arrhenius expression (Equation (S6)) utilizing the reaction rate constants calculated from Equation (S5).

$$\ln\big(k(T)\big) - \ln(k_1) = -\frac{E_a}{R}\left(\frac{1}{T} - \frac{1}{T_1}\right) \tag{S6}$$

Here $k(T)$ is the rate constant at the temperature T in the reactor. T_1 is the lowest temperature at which conversion was measured, and k_1 the rate constant at T_1. R is the universal gas constant (8.31447 J/K/mol). The pre-exponential factor was subsequently calculated from Equation (S7).

$$k_1 = k_0 \cdot \exp\left(-\frac{E_a}{RT_1}\right) \quad \text{(S7)}$$

Where k_0 is the pre-exponential factor.

2. Results

2.1. Characterization

2.1.1. XRD

The fresh catalyst samples and some of the supports were characterized by XRD. For the catalysts containing hydroxyapatite (Figure S1) the loading of V_2O_5 and Nb_2O_5 was below the detection limit and the oxides were probably dispersed as amorphous monolayers not visible by XRD.

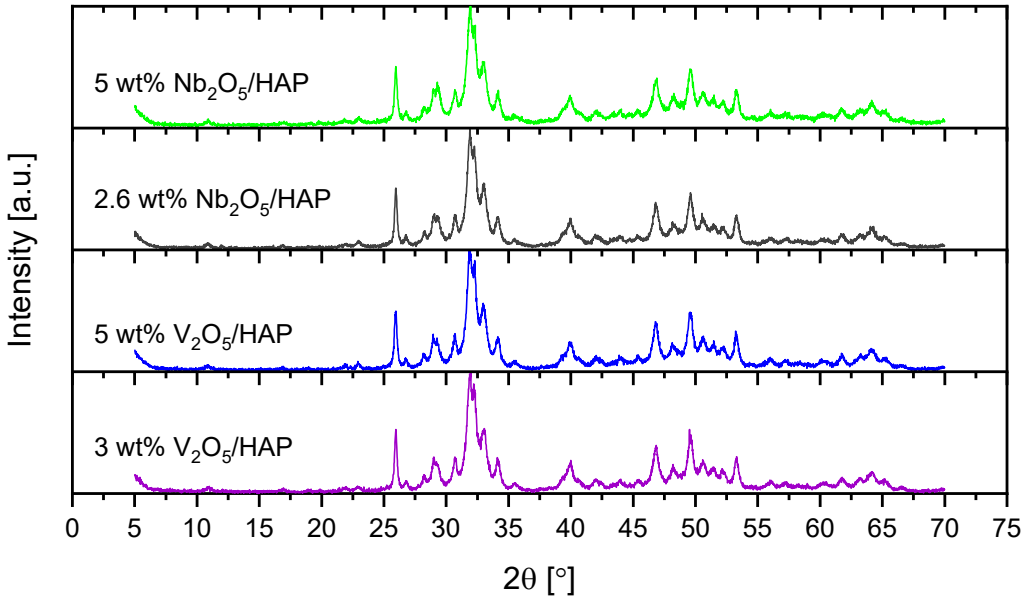

Figure S1. XRD diffractograms measured for the catalyst samples supported on the commercial hydroxyapatite (HAP).

For the V_2O_5/HAP and Nb_2O_5/HAP only three different calcium phosphate phases were found, however, there was an increase in the amount of β-$Ca_2P_2O_7$ in the catalysts with higher loading, indicating the formation of $Ca_3(VO_4)_2$ and $Ca_3(NbO_4)_2$ or a temperature dependence on the calcium phosphate phases.

For the catalysts supported on α-Al_2O_3 (Figure S2) only the high loading MoO_3 showed any features different from the support, thus, only α-Al_2O_3 (D = 1000 Å) was detected by XRD for the other samples. For the 6.2 wt% MoO_3/α-Al_2O_3 3.8 wt% α-MoO_3 (orthorhombic, D = 485 Å) was measured, which were lower than the expected composition, probably due to the difficulty to detect small particles and dispersed amorphous phases with XRD.

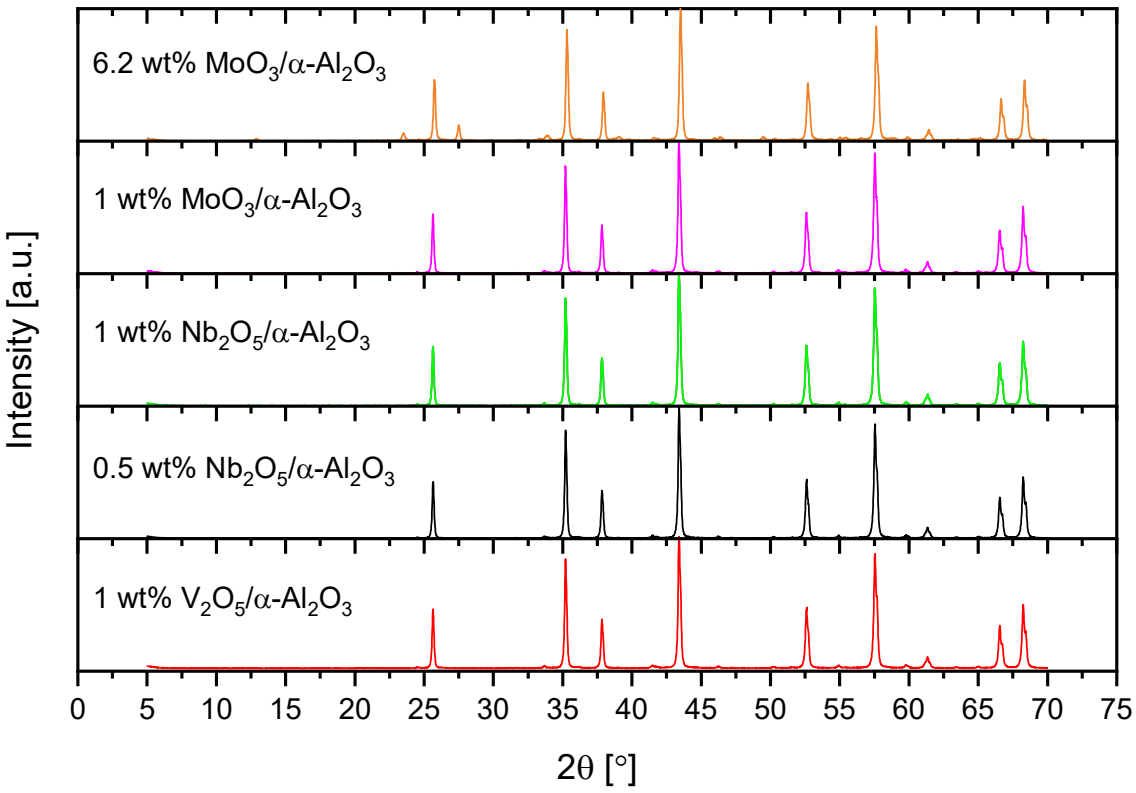

Figure S2. XRD diffractograms measured for the catalyst samples supported on α-Al_2O_3.

The antimony containing samples were not easily described from their XRD diffractograms (Figure S3). Thus, there were no phases identified with certainty for the V-Sb-O sample, but suggested phases were $SbO_5 \cdot 1.5H_2O$ and VO_2. For the Mo-Sb-O sample, MoO_2 and Sb_6O_{13} were identified, but there were multiple undefined phases present, thus, the quantification was only relative, with 28 wt% MoO_2 and 72 wt% Sb_6O_{13}. For the SbO/SiO_2 XRD gave 97.7 wt% amorphous SiO_2 and 2.3 wt% Sb_2O_4, but with large uncertainty due to the amorphous material. The XRD measurements thus did not give much information.

The evolution of the vanadyl phosphate through the preparation described in Section 1.1.3.2 was observed in the XRD diffractograms (Figure S4).

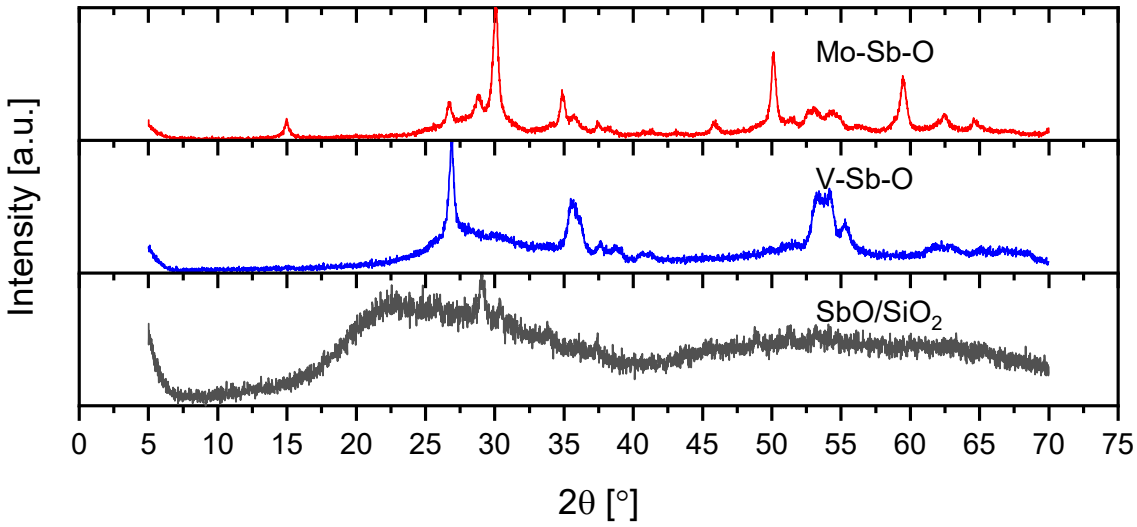

Figure S3. XRD diffractograms measured for the antimony containing samples.

After the first reflux, $VOPO_4 \cdot 2H_2O$ was obtained as described by Behera et al. [2] and was confirmed to be phase pure by XRD (tetragonal, D = 1525 Å). When calcined at 400°C, VPO (a) was obtained. No phase change was measured, but the crystal size decreased from 1525 Å before calcination to 235 Å after calcination, contrary to expectations due to sintering at higher temperatures. The $VOPO_4 \cdot 2H_2O$ was further refluxed in isobutanol, in agreement with Behera et al. [2] $VOHPO_4 \cdot 0.5H_2O$ was obtained (monoclinic, D = 465 Å). After reflux in water and calcination of $VOHPO_4 \cdot 0.5H_2O$, VPO (b) was produced. The XRD analysis was not conclusive on the phases, but with the best matches being $VOHPO_4 \cdot 0.5H_2O$ and $VOPO_4 \cdot 2H_2O$, though H_2O was expected to evaporate during calcination. The diffractogram was substantially different from the diffractograms of the three other measured VPO samples (15a, $VOHPO_4 \cdot 0.5H_2O$ and $VOPO_4 \cdot 2H_2O$).

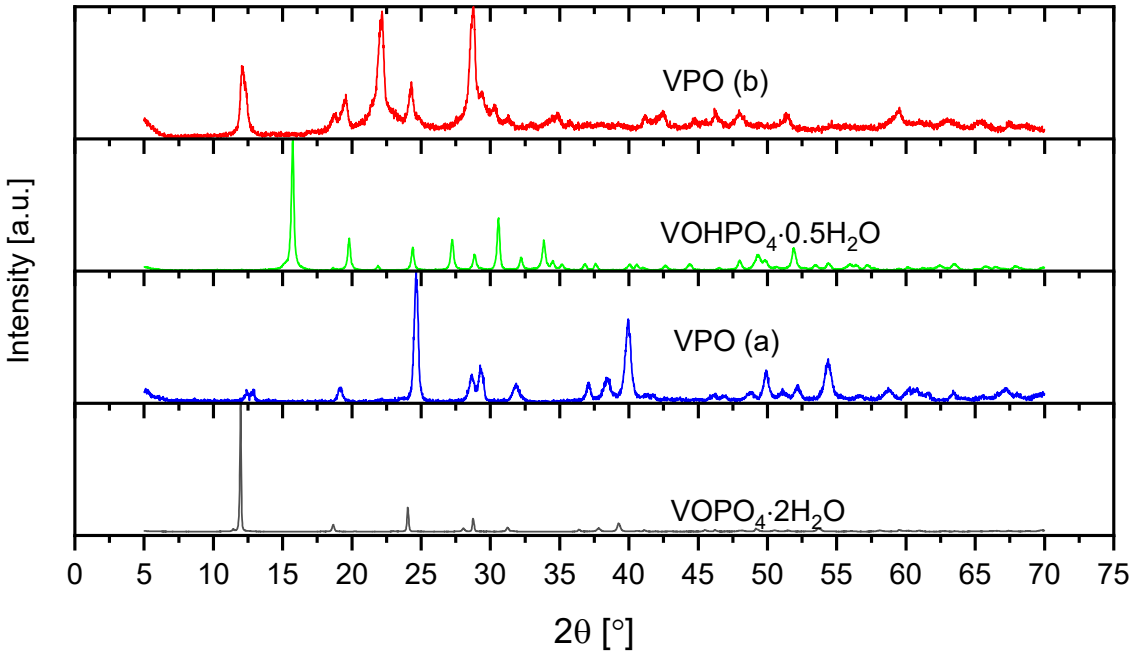

Figure S4. XRD diffractogram measured for the vanadyl phosphate samples. VPO (a) was when the $VOPO_4 \cdot 2H_2O$ sample, obtained after the first reflux, was calcined. VPO (b) was when the $VOHPO_4 \cdot 0.5H_2O$ sample, obtained after additional refluxes in isobutanol and water, was calcined.

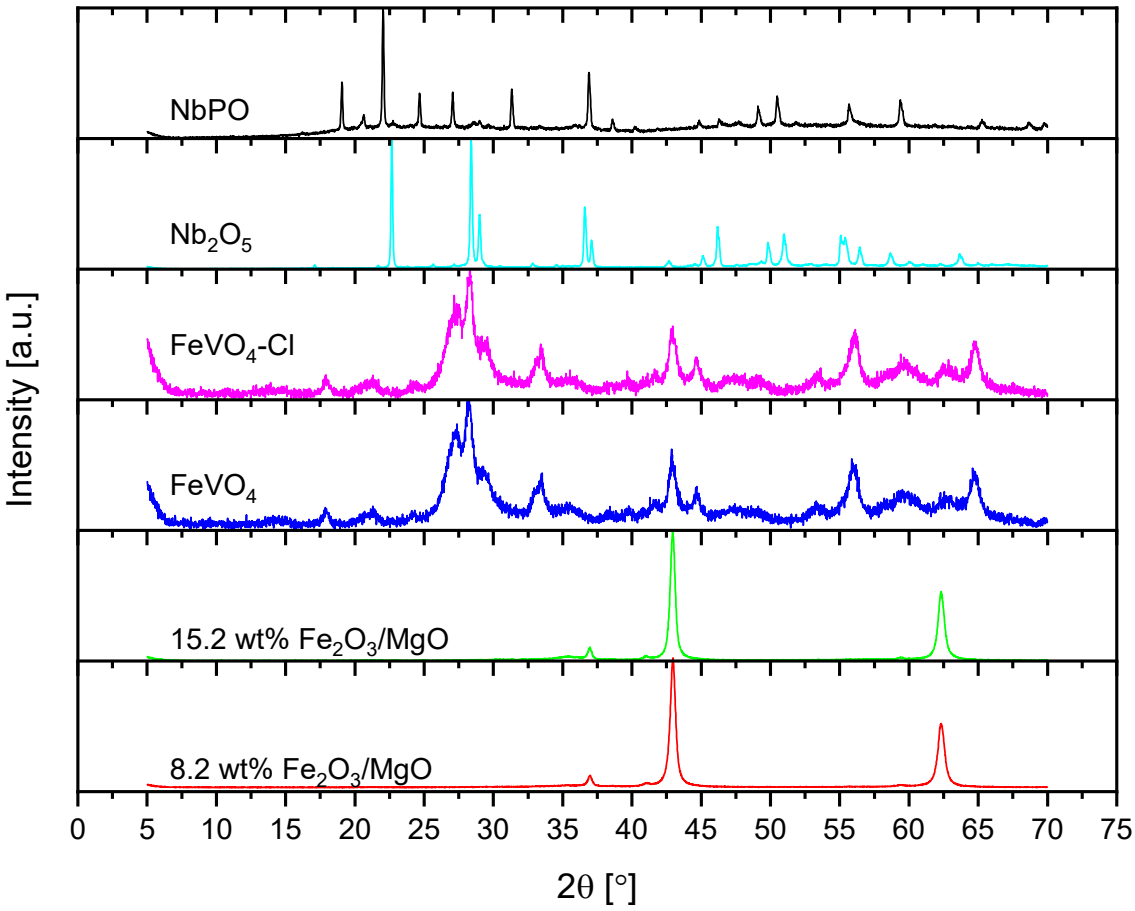

Figure S5. XRD diffractograms for NbPO, $FeVO_4$ and Fe_2O_3/MgO samples.

As expected, the Fe_2O_3/MgO consisted mostly of MgO (95.5 wt%, D = 247 Å, for the 8.2 wt% and 91 wt%, D = 284 Å for the 15.2 wt%) (Figure S5). However, iron was only oxidized to Fe_3O_4 (magnetite) (4.5 wt%, cubic, D = 40 Å for the 8.2 wt% and 9 wt%, D = 50 Å for the 15.2 wt%) and not Fe_2O_3 and the weight fractions of MgO was higher than expected. The diffractogram for Nb_2O_5 treated in phosphoric acid (Figure S5) was close to Nb_2O_5, with a small amount of NbO_2 and possibly some $H_4P_2O_7$, as the fit was uncertain. Thus, niobium phosphate was not the product of this preparation method. The $FeVO_4$ diffractogram was a mixture of Fe_4V, $V_{0.9}Fe_{0.1}$, VO_2 and V_2O_3 phases with some undetermined peaks, and the same was observed when promoted with 1 wt% Cl, which was not observed in XRD. $FeVO_4$ as pure phase was thus not achieved.

2.1.2. BET

The BET surface area was measured on the HAP and α-Al_2O_3 supports and on all catalyst samples (Table S4).

Table S4. Overview of BET surface areas measured on the catalysts tested.

#	Type	SSA [m²/g]		#	Type	SSA [m²/g]
1	8.2 wt% Fe_2O_3/MgO	60.4		12	0.5 wt% Nb_2O_5/α-Al_2O_3	9.2
2	15.2 wt% Fe_2O_3/MgO	35.1		13	SbO/SiO_2	167.5
3	3.0 wt% V_2O_5/HAP	66.6		14	Nb_2O_5	6.2
4	5 wt% V_2O_5/HAP	60.9		15a	VPO	4.8
5	2.6 wt% Nb_2O_5/HAP	66.6		15b	VPO	22.3
6	5 wt% Nb_2O_5/HAP	62.8		16	$FeVO_4$	55.4
7	6.2 wt% MoO_3/α-Al_2O_3	9.2		17	$FeVO_4$-1 wt% Cl	52.9
8	1 wt% MoO_3/α-Al_2O_3	9.3		18	V-Sb-O	18.7
9	1 wt% V_2O_5/α-Al_2O_3	9.9		19	Mo-Sb-O	42.4
10	0.5 wt% Nb_2O_5/α-Al_2O_3	9.2		20	NbPO	10.1
11	1 wt% Nb_2O_5/α-Al_2O_3	9.6				
	HAP	103.5			α-Al_2O_3	8.3

The surface areas of the tested catalysts vary much (Table S4), where the catalyst with the lowest surface area was the vanadium phosphate (#15a, 4.8 m²/g), which was only refluxed in ortho-phosphoric acid. The subsequent step of reflux in isobutanol increased the surface area by a factor of 3.5 (15b, 22.3 m²/g). The surface area of the HAP supported catalysts were mostly similar for the vanadium and niobium samples. The specific surface area decreased with increased metal oxide loading. Comparing the surface area of HAP (Table S4) with the impregnated samples (Table S4) the surface area strongly decreased from the impregnation and calcination. The surface area of the α-Al_2O_3 was slightly lower than the corresponding impregnated samples.

2.1.3. ICP

Elemental analysis was performed on filtered samples (Table S5), as some of the material may be lost with the filtrate.

Table S5. Results of elemental analysis for catalysts samples, which were filtered during the preparation.

#	Sample	V	P	Fe	Nb	Mo	Sb
		[wt%]	[wt%]	[wt%]	[wt%]	[wt%]	[wt%]
15a	VPO	25.3	15.6	-	-	-	-
15b	VPO	27.5	17.0	-	-	-	-

14	Nb_2O_5	-	-	-	71.6	-	-
18	V-Sb-O	3	-	-	-	-	74
19	Mo-Sb-O	-	-	-	-	5	75

No phosphorous was measured in #14 (Table S5) though the preparation method was similar to the preparation of #15a and was done with the $NbCl_5$ as raw material as in the literature [12,13]. This agreed with the XRD results, thus Nb_2O_5 was obtained from the reflux method. The molar ratio of both the vanadium phosphate samples (15a and 15b) were V/P = 0.56. Thus, there was almost the double amount of phosphate to vanadium.

For the co-precipitated samples (#18 and #19) the stoichiometric ratios V/Sb and Mo/Sb were calculated to be 0.056 and 0.085. Hence, for #18 the actual nominal V_2O_5 loading were 5.4 wt% and for #19 the actual nominal MoO_3 loading was 7.5 wt%.

2.2. Testing of Powder Catalysts

The measurements were done with a loading of 0.05 g catalyst if nothing else is stated below. The feed consisted of ~150 NmL/min, 3-5% MeOH and 10% O_2 in N_2. The results are summarized and compared with an industrial reference (FeMo, $MoO_3/Fe_2(MoO_4)_3$) in the following sections. If nothing else is stated, the selectivity reported is the DME corrected selectivity, as this was a good performance indicator since DME was a reversible product, and thus may still be converted to formaldehyde.

2.2.1. Molybdenum Containing Catalysts

For the initial screenings, four different catalysts containing molybdenum were tested: 6.2 wt% MoO_3/α-Al_2O_3, 1 wt% MoO_3/α-Al_2O_3, Mo-Sb-O and 10 wt% MoO_3/MgO (Figure S6). They were all less active than the FeMo catalyst (Figure S6b), but the selectivity was high except for the 10 wt% MoO_3/MgO catalyst (Figure S6a,c), as expected for a basic oxide.

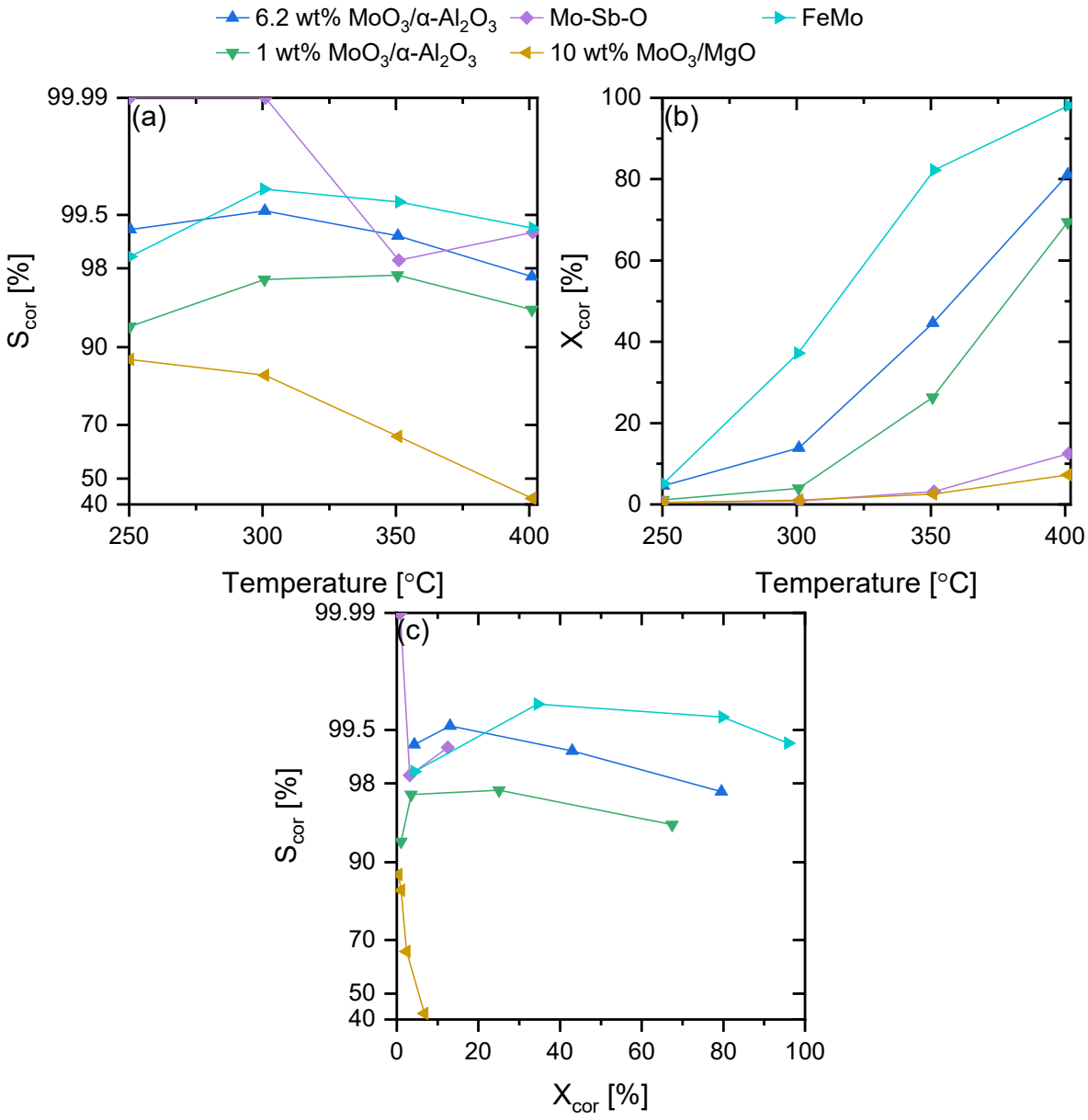

Figure S6. Screening results for molybdenum containing catalysts. FeMo included for comparison. 50 mg of catalyst in a feed of 3-5% MeOH in 127.5 NmL/min N_2 and 15 NmL/min O_2. (a) S_{cor} vs. temperature, (b) X_{cor} vs. temperature and (c) S_{cor} vs. X_{cor}.

The full product distribution and the rate constants were also determined at the different temperatures (Table S6).

Table S6. Selectivities at 250-400°C, conversion and reaction rate constants for the fresh molybdenum containing catalysts with 50 mg of catalyst, in a feed flow of 15 NmL/min O_2, 127.5 NmL/min N_2 and 3-5% CH_3OH.

#	Sample	T_{sp}	k	X	S_i [%]			
		[°C]	[L/(m²s)]	[%]	CH_2O	DME	CO	CO_2
7	6.2 wt% MoO_3/α-Al_2O_3	250	$3.4 \cdot 10^{-4}$	4.6	94.4	4.9	0.0	0.7
		300	$1.2 \cdot 10^{-3}$	13.9	93.7	5.9	0.0	0.4
		350	$5.0 \cdot 10^{-3}$	44.6	95.4	3.8	0.7	0.2
		400	$1.5 \cdot 10^{-2}$	81.1	95.8	1.8	2.2	0.2
8	1 wt% MoO_3/α-Al_2O_3	250	$7.9 \cdot 10^{-5}$	1.2	85.6	8.0	0.0	6.3
		300	$3.0 \cdot 10^{-4}$	3.9	88.0	9.6	0.0	2.3
		350	$2.5 \cdot 10^{-3}$	26.5	93.0	4.8	1.5	0.7
		400	$3.0 \cdot 10^{-2}$	69.4	92.4	2.8	3.4	1.4
12	10 wt% MoO_3/MgO	250	$3.7 \cdot 10^{-6}$	0.4	87.7	0.0	0.0	12.3
		300	$9.3 \cdot 10^{-6}$	1.1	84.4	0.0	0.0	15.6
		350	$2.4 \cdot 10^{-5}$	2.5	62.3	5.5	9.5	22.7
		400	$7.5 \cdot 10^{-5}$	7.2	39.6	6.5	20.3	33.6
19	Mo-Sb-O	250	$9.4 \cdot 10^{-6}$	0.5	100	0.0	0.0	0.0
		300	$1.8 \cdot 10^{-5}$	0.9	100	0.0	0.0	0.0
		350	$7.0 \cdot 10^{-5}$	3.1	98.4	0.0	0.0	1.6
		400	$3.2 \cdot 10^{-4}$	12.5	99.2	0.0	0.0	0.8

The selectivity towards DME mostly decreased with increasing temperature and conversion, yielding higher formaldehyde selectivity. This emphasized, that the DME corrected selectivity was a good descriptor of the catalysts performance, however, it is not desirable, that the DME selectivity is too high, which was not the case for any of the molybdenum containing catalysts. The 6.2 wt% MoO_3/α-Al_2O_3 and 1 wt% MoO_3/α-Al_2O_3 lost 36% and 32% of the initial activity at 400°C within 8 h and were thus not very stable. Similarly the Mo-Sb-O catalyst lost 58% of its activity. An Arrhenius plot was made (Figure S7) and the pre-exponential factors and activation energies were calculated for the fresh catalysts (Table S7).

The 10 wt% MoO_3/MgO and the Mo-Sb-O catalyst had both low activation energy and pre-exponential factor, thus, even at elevated temperatures they would not be active, and thus not of interest (Figure S7).

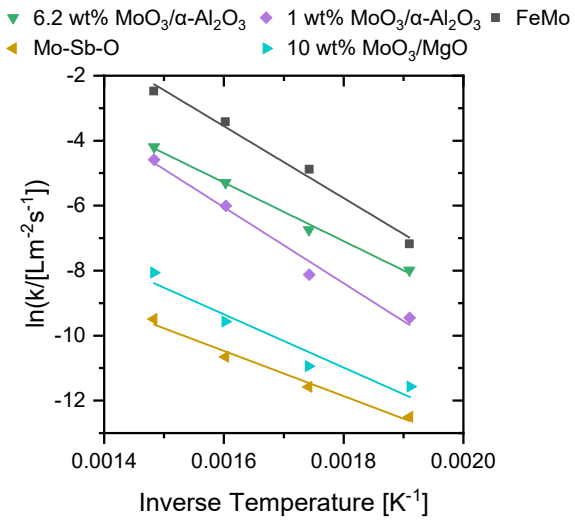

Figure S7. Arrhenius plot for molybdenum containing catalysts.

Table S7. Pre-exponential factor (k_0) and activation energy (E_a) of molybdenum containing catalysts.

#	Sample	k_0	E_a
		[L/(m²s)]	**[kJ/mol]**
7	6.2 wt% MoO_3/α-Al_2O_3	$9.3 \cdot 10^3$	75.0
8	1 wt% MoO_3/α-Al_2O_3	$3.2 \cdot 10^5$	97.2
12	10 wt% MoO_3/MgO	$1.9 \cdot 10^0$	57.8
19	Mo-Sb-O catalyst	$4.6 \cdot 10^1$	68.1

2.2.2. Vanadium Containing Catalysts

The vanadium containing catalysts tested were 5 wt% V_2O_5/HAP, 3 wt% V_2O_5/HAP, two vanadium phosphates, 1 wt% V_2O_5/α-Al_2O_3, $FeVO_4$, $FeVO_4$ doped with 1 wt% Cl, 3 wt% V_2O_5/MgO and V-Sb-O catalyst (Figure S8). Several of the vanadium containing catalyst samples were more active than the FeMo catalyst. However, they showed decreasing selectivity at increasing temperature (Figure S8a), except for the vanadium phosphates and V-Sb-O catalyst, which had low conversions. The V-Sb-O catalyst had increased selectivity with temperature, which was in agreement with Zhang et al. [14] for mixed V-Sb oxide supported on SiO_2. Comparing the VPO catalysts with the literature, Behera et al. [1,2] had reported selectivities of above 95% for WO_3 promoted vanadium phosphate at up to 300°C. Whiting et al. [15] reported selectivities of 93% and above at 200°C and 400°C for vanadium containing molybdenum phosphates. For the $VOHPO_4 \cdot 0.5H_2O$ the selectivity to formaldehyde was reported lower than for $VOPO_4 \cdot 2H_2O$, but opposite for the activity. This was also obtained for the calcined vanadium phosphates in this study (Figure S8).

The $FeVO_4$ and $FeVO_4$-Cl samples were tested with only 7.5 mg of catalyst loaded in the reactor due to very high activity. The selectivity of the $FeVO_4$ was 90% at 300°C and 350°C in agreement

with the Andersson group [16–19], but fell in selectivity at 400°C when full conversion was reached (Figure S8a,c). $FeVO_4$ was doped with 1 wt% of Cl to decrease the surface basicity of the sample, as done by Wang and Wachs [20] who showed that the selectivity could be moved from acidic by-products (DME and DMM) to formaldehyde or all the way to basic by-products (CO_2) by promotion with K_2O. Alkali-metals are often used to passivate Brønsted acidity [21], and it was considered that halogens may similarly passivate basicity. The selectivity was improved from 91% to 99% towards formaldehyde at 300°C and from 91% to 94% at 350°C for the $FeVO_4$ after doping with Cl (Figure S8a). The full results for the selectivities and the calculated rate constants achieved in the powder tests are shown in Table S8. In addition it can be mentioned, that the VPO catalysts were stable over 8 h on stream at 400°C, and that the V-Sb oxide catalyst lost 35% of its activity under the same conditions.

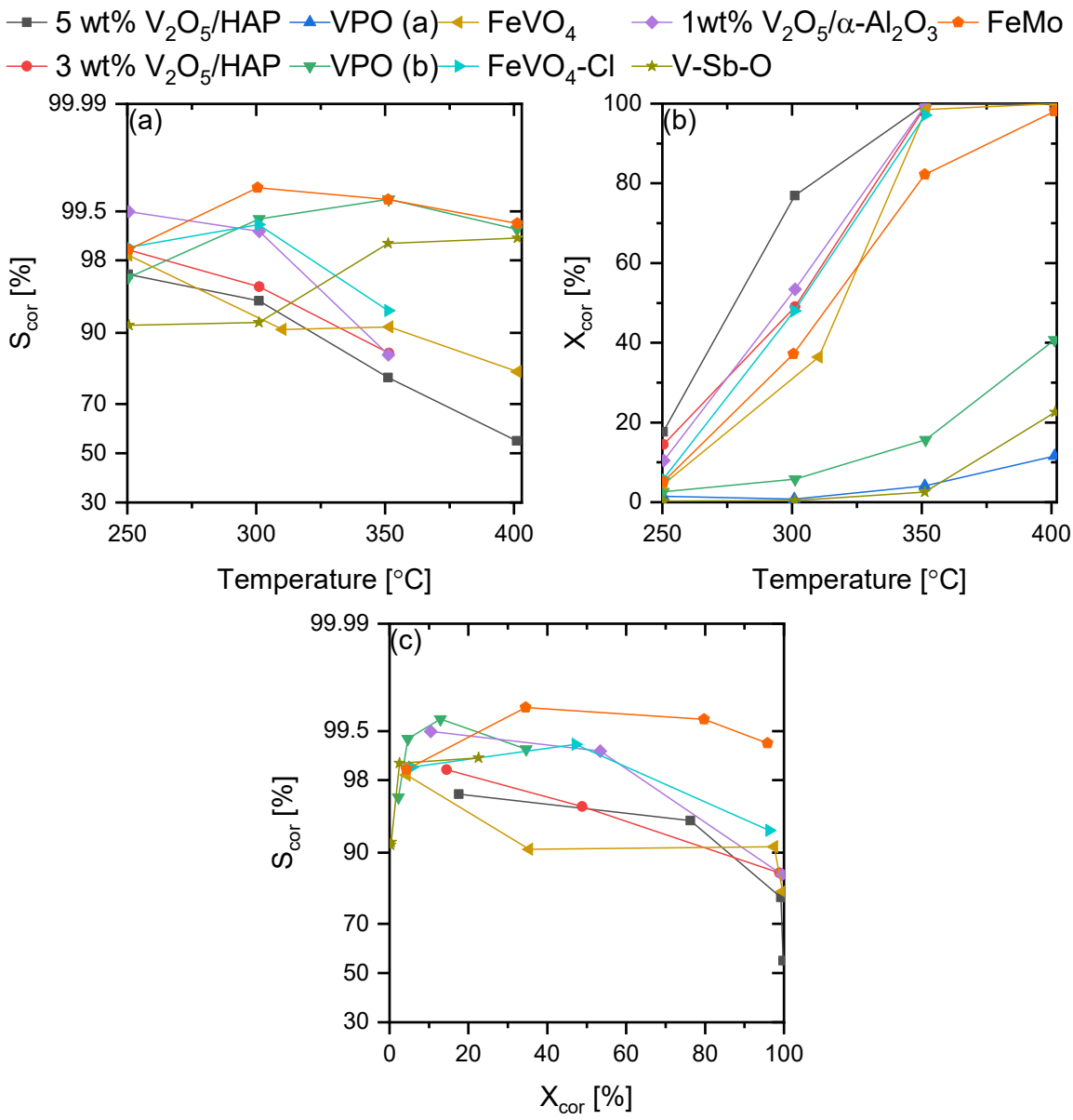

Figure S8. Screening results for vanadium containing catalysts. FeMo included for comparison. 50 mg of catalyst (except for the $FeVO_4$ samples, here it was 7.5 mg) in a feed of 3-5% MeOH in 127.5 NmL/min N_2 and 15 NmL/min O_2. (a) S_{cor} vs. temperature, (b) X_{cor} vs. temperature and (c) S_{cor} vs. X_{cor}.

Table S8. Selectivities at 250-400°C, conversion and reaction rate constants for the vanadium containing catalysts with 50 mg of catalyst (except $FeVO_4$ and $FeVO_4$-Cl which were tested with 7.5 mg), in a feed flow of 15 NmL/min O_2, 127.5 NmL/min N_2 and 3-5% CH_3OH.

#	Sample	T_{sp}	k	X	S_i [%]			
		[°C]	[L/(m²s)]	[%]	CH_2O	DME	CO	CO_2

3	3 wt% V_2O_5/HAP	250	$1.7 \cdot 10^{-4}$	14.5	98.5	0.0	0.0	1.5
		300	$7.9 \cdot 10^{-4}$	49.0	95.7	0.5	1.5	2.3
		350	-	99.4	85.3	0.5	11.9	2.4
		400	-	99.8	65.4	0.1	31.0	3.5
4	5 wt% V_2O_5/HAP	250	$1.6 \cdot 10^{-4}$	17.6	96.6	0.6	0.7	2.2
		300	$1.4 \cdot 10^{-3}$	76.9	94.0	0.8	3.4	1.8
		350	-	99.8	78.5	0.5	19.3	1.6
		400	-	100	55.1	0.2	42.3	2.4
9	1 wt% V_2O_5/α-Al_2O_3	250	$7.0 \cdot 10^{-4}$	10.5	99.5	0.0	0.0	0.5
		300	$5.2 \cdot 10^{-3}$	53.4	99.1	0.0	0.5	0.4
		350	-	99.5	85.3	0.0	13.5	1.1
		400	-	100	60.6	0.0	37.0	2.4
15a	VPO	250	$2.3 \cdot 10^{-4}$	1.5	100	0.0	0.0	0.0
		300	$1.3 \cdot 10^{-4}$	0.8	86.1	13.9	0.0	0.0
		350	$7.4 \cdot 10^{-4}$	4.1	88.6	11.4	0.0	0.0
		400	$2.3 \cdot 10^{-3}$	11.6	91.7	8.3	0.0	0.0
15b	VPO	250	$8.7 \cdot 10^{-5}$	2.6	84.3	13.1	0.0	2.7
		300	$2.1 \cdot 10^{-4}$	5.8	79.9	19.6	0.0	0.5
		350	$6.4 \cdot 10^{-4}$	15.7	81.8	17.9	0.0	0.3
		400	$2.1 \cdot 10^{-3}$	40.7	84.4	14.9	0.6	0.1
16	$FeVO_4$	250	$3.6 \cdot 10^{-4}$	4.5	94.3	4.0	0.0	1.7
		300	$3.9 \cdot 10^{-3}$	36.4	88.2	2.7	8.9	0.3
		350	$3.8 \cdot 10^{-2}$	98.5	90.2	1.0	8.6	0.2
		400	-	100	80.5	0.3	18.7	0.5
17	$FeVO_4$-Cl	250	$4.6 \cdot 10^{-4}$	5.9	95.5	3.1	0.0	1.4
		300	$5.4 \cdot 10^{-3}$	48.1	97.5	1.8	0.5	0.2
		350	$3.2 \cdot 10^{-2}$	97.1	92.7	0.9	6.2	0.2
		400	-	100	81.4	0.6	17.6	0.4
18	V-Sb-O	250	$1.3 \cdot 10^{-5}$	0.3	91.3	0.0	0.0	8.7
		300	$1.8 \cdot 10^{-5}$	0.4	91.8	0.0	0.0	8.2
		350	$1.3 \cdot 10^{-4}$	2.6	98.7	0.0	0.0	1.3
		400	$1.3 \cdot 10^{-3}$	22.6	98.9	0.0	0.0	1.1

The pre-exponential factors and activation energies were calculated using the Arrhenius equation (Figure 9, Table S9). The vanadium containing catalysts differed much more in the activation energy compared to the molybdenum containing catalysts (Table S7). The vanadium phosphates

had much lower activation energies and pre-exponential factors than the other vanadium samples. Though, the fit of the vanadium phosphate (a) was poor since the measurement at 250°C gave a higher conversion and reaction rate than the measurement at 300°C (Table S8 and Figure 9) probably due to measurement uncertainty due to the low product concentrations.

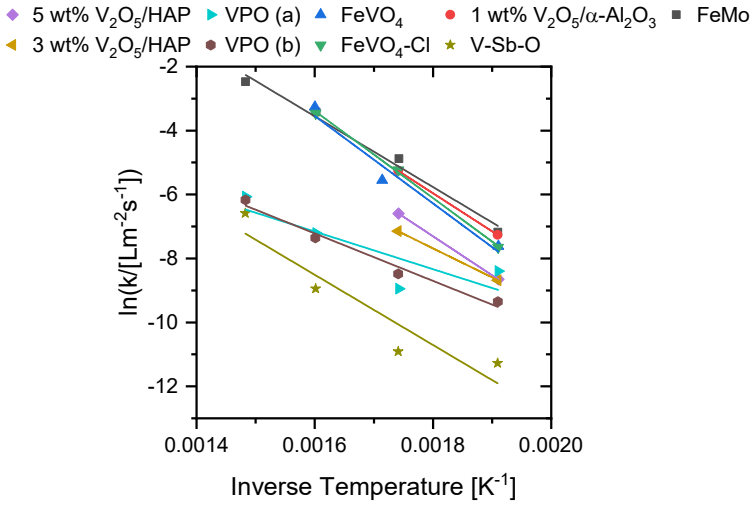

Figure S9. Arrhenius plot for vanadium containing catalysts.

Table S9. Pre-exponential factor (k_0) and activation energy (E_a) of vanadium containing catalysts.

#	Sample	k_0	E_a
		[L/(m²s)]	[kJ/mol]
3	3 wt% V_2O_5/HAP	$5.8 \cdot 10^3$	75.5
4	5 wt% V_2O_5/HAP	$2.3 \cdot 10^6$	101.5
9	1.0 wt% V_2O_5/α-Al_2O_3	$5.3 \cdot 10^6$	99.1
15a	VPO	$1.1 \cdot 10^1$	48.9
15b	VPO	$1.1 \cdot 10^2$	61.7
16	$FeVO_4$	$5.7 \cdot 10^8$	122.7
17	$FeVO_4$-Cl	$1.6 \cdot 10^8$	115.4
18	V-Sb-O	$1.0 \cdot 10^4$	91.3

2.2.3. Alternative Catalysts

The last group of catalysts was those not containing either molybdenum or vanadium. These included Fe_2O_3/MgO, Nb_2O_5/HAP, Nb_2O_5/α-Al_2O_3, Nb_2O_5, SbO/SiO_2 and NbPO (Figure S10).

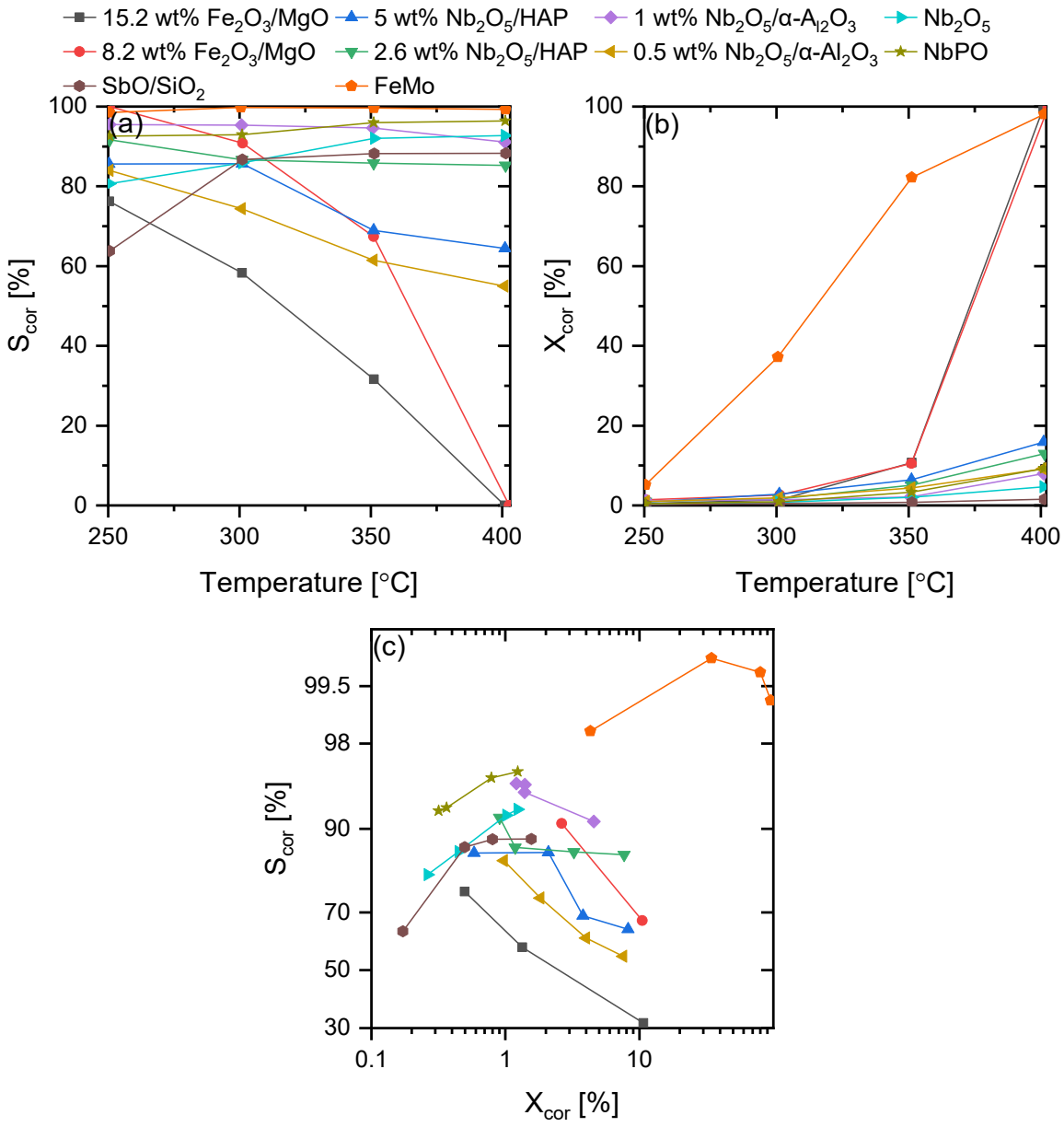

Figure S10: Screening results for alternative catalysts not containing molybdenum or vanadium. FeMo included for comparison. 50 mg of catalyst in a feed of 3-5% MeOH in 127.5 NmL/min N_2 and 15 NmL/min O_2. (a) S_{cor} vs. temperature, (b) X_{cor} vs. temperature and (c) S_{cor} vs. X_{cor}.

All the alternative catalyst not containing Mo and V were much less active than the FeMo catalyst (Figure S10b), except for the 8.2 and 15.2 wt% Fe_2O_3/MgO catalysts at 400°C, but here the selectivity was exclusively towards CO and CO_2 (Figure S10a). This was not in agreement with the results reported by El-Molla and Mahmoud [22] for a 15.2 wt% Fe_2O_3/MgO catalyst prepared

similarly. El-Molla and Mahmoud [22] reported a selectivity of 96.2% at 400°C and 29% conversion. It is not clear whether there were oxygen in the feed or not, which may explain why the results differ from the results over similar catalysts. The conversions reported here were higher, which may have influenced the selectivity results. The selectivity was also low at low temperatures, where the conversion was still low. For the Nb_2O_5/HAP the increase from 2.6 wt% to 5 wt% Nb_2O_5 decreased the selectivity, while an increase from 0.5 wt% to 1 wt% on the α-Al_2O_3 increased selectivity (Figure S10a and c). The SbO/SiO_2 increased in selectivity towards fomaldehyde with increased temperature, as for the V-Sb-O catalyst. In both cases the remaining selectivity was towards CO_2, which may have been falsely high at low temperatures due to better sensitivity for CO_2 and very low conversions. This can probably be attributed to the activity of the antimony oxide component. The activity of the SbO/SiO_2 was very low, despite the high surface area of 167.5 m^2/g. This was partly in agreement with Abadzhieva and Klissurski [23] who reported Sb_2O_4 to be an order of magnitude less active than MoO_3, but also to reach maximum activity and selectivity at 500°C. Sb_2O_4 was reported to increase the stability of commercial catalysts [24], however, after the short time on stream during the test, a yellowish deposit was observed at the reactor outlet from the SbO/SiO_2. This indicates, that antimony oxide is probably not of much use to stabilize against volatilization.

For NbPO catalyst, selectivities of 90% towards formaldehyde at high conversions was reported by Davies and Taylor [12,13]. The DME corrected selectivity found in this study was above 90%, at 250-400°C but conversion was below 15% and the selectivity may decrease at higher conversions.

The full results for the catalysts not containing molybdenum or vanadium are shown in Table S10.

The Fe_2O_3/MgO systems did not make any DME, which was not surprising as DME is known to be acid catalyzed and neither iron oxide or MgO are acidic oxides. The antimony oxide supported on silica also did not yield DME. The niobium containing catalysts on the other hand had high selectivity to DME, as expected [20,25,26], making them less interesting as potential catalysts, even though the DME corrected selectivity was around 90% for most of them. Comparing the 0.5 wt% and 1 wt% Nb_2O_5/α-Al_2O_3 catalysts, there was much less DME produced on the 0.5 wt% sample and much more CO_2. However, for the HAP systems, the 5 wt% Nb_2O_5 sample produced much more CO_2 and less CH_2O compared to the 2.5 wt% Nb_2O_5/HAP.

Pre-exponential factors and activation energies were calculated from the Arrhenius expression (Figure 11 and Table S11). All the investigated samples, which did not contain molybdenum or vanadium had low pre-exponential factors (especially the SbO/SiO_2 catalyst catalyst).

Table S10. Specific selectivities at 250-400°C, conversion and reaction rate constants for the catalysts not containing molybdenum or vanadium with 50 mg of catalyst, in a feed flow of 15 NmL/min O_2, 127.5 NmL/min N_2 and 3-5% CH_3OH.

#	Sample	T_{sp}	k	X	S_i [%]			
		[°C]	[L/(m²s)]	[%]	CH_2O	DME	CO	CO_2
1	8.2 wt% Fe_2O_3/MgO	250	$1.6 \cdot 10^{-5}$	1.4	100	0.0	0.0	0.0
		300	$3.4 \cdot 10^{-5}$	2.6	90.8	0.0	0.0	9.2
		350	$1.5 \cdot 10^{-4}$	10.5	67.4	0.0	10.2	22.4
		400	-	99.7	0.0	0.0	10.8	89.2
2	15.2 wt% Fe_2O_3/MgO	250	$9.0 \cdot 10^{-6}$	0.5	76.2	0.0	0.0	23.8
		300	$2.7 \cdot 10^{-5}$	1.3	58.3	0.0	0.0	41.7
		350	$2.4 \cdot 10^{-4}$	10.7	31.6	0.0	22.2	46.3
		400	-	99.8	0.0	0.0	5.8	94.2
5	2.6 wt% Nb_2O_5/HAP	250	$8.7 \cdot 10^{-6}$	1.0	86.8	5.3	0.0	7.9
		300	$1.5 \cdot 10^{-5}$	1.6	62.5	27.9	0.0	9.6
		350	$5.2 \cdot 10^{-5}$	5.1	54.6	36.3	0.0	9.0
		400	$1.5 \cdot 10^{-4}$	13.0	50.7	40.6	1.5	7.2
6	5 wt% Nb_2O_5/HAP	250	$8.2 \cdot 10^{-6}$	0.9	57.5	32.8	0.0	9.7
		300	$2.8 \cdot 10^{-5}$	2.8	64.2	25.1	0.0	10.7
		350	$7.0 \cdot 10^{-5}$	6.4	40.6	41.1	0.0	18.3
		400	$1.9 \cdot 10^{-4}$	15.9	33.4	48.2	1.7	16.7
10	0.5 wt% Nb_2O_5/α-Al_2O_3	250	$6.6 \cdot 10^{-5}$	1.0	84.0	0.0	0.0	16.0
		300	$1.4 \cdot 10^{-4}$	1.9	71.4	3.9	0.0	24.6
		350	$3.6 \cdot 10^{-4}$	4.3	56.5	8.1	0.0	35.4
		400	$8.4 \cdot 10^{-4}$	9.2	45.4	17.4	2.6	34.6
11	1 wt% Nb_2O_5/α-Al_2O_3	250	$7.6 \cdot 10^{-5}$	1.2	95.5	0.0	0.0	4.5
		300	$9.6 \cdot 10^{-5}$	1.4	95.4	0.0	0.0	4.6
		350	$1.6 \cdot 10^{-4}$	2.1	62.0	34.5	0.0	3.5
		400	$6.6 \cdot 10^{-4}$	8.0	52.0	42.9	3.5	1.5
13	SbO/SiO_2	250	$6.2 \cdot 10^{-7}$	0.2	63.8	0.0	0.0	36.2
		300	$1.8 \cdot 10^{-6}$	0.5	86.8	0.0	0.0	13.2
		350	$3.0 \cdot 10^{-6}$	0.8	88.2	0.0	0.0	11.8
		400	$6.1 \cdot 10^{-6}$	1.6	88.3	0.0	0.0	11.7
14	Nb_2O_5	250	$2.7 \cdot 10^{-5}$	0.3	80.6	0.0	0.0	19.4
		300	$8.6 \cdot 10^{-5}$	0.8	49.7	42.1	0.0	8.2
		350	$2.5 \cdot 10^{-4}$	2.0	45.9	50.1	0.0	4.0
		400	$6.1 \cdot 10^{-4}$	4.6	24.7	73.4	0.0	1.9
20	NbPO	250	$3.4 \cdot 10^{-5}$	0.4	68.0	26.5	0.0	5.5
		300	$8.3 \cdot 10^{-5}$	1.0	35.6	61.7	0.0	2.7

		350	$3.2 \cdot 10^{-4}$	3.3	23.0	76.0	0.0	1.0
		400	$9.9 \cdot 10^{-4}$	9.3	12.9	86.7	0.0	0.5

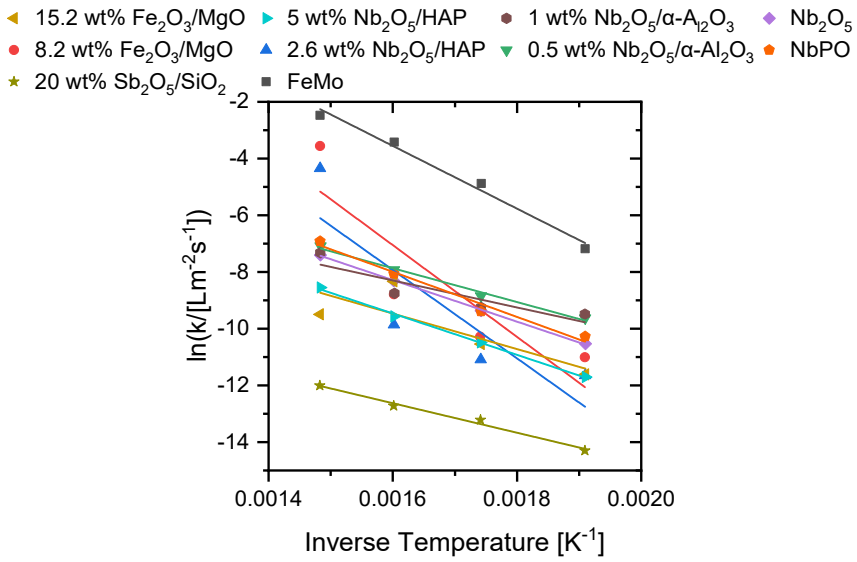

Figure S11. Arrhenius plot for catalysts not containing molybdenum or vanadium.

Table S11. Pre-exponential factor (k_0) and activation energy (E_a) of catalysts not containing molybdenum or vanadium.

#	Sample	k_0	E_a
		[L/(m²s)]	[kJ/mol]
1	8.2 wt% Fe_2O_3/MgO	$1.2 \cdot 10^{1}$	59.3
2	15.2 wt% Fe_2O_3/MgO	$4.1 \cdot 10^{3}$	87.5
5	2.6 wt% Nb_2O_5/HAP	$2.7 \cdot 10^{0}$	56.0
6	5 wt% Nb_2O_5/HAP	$9.1 \cdot 10^{1}$	60.6
10	0.5 wt% Nb_2O_5/α-Al_2O_3	$5.4 \cdot 10^{0}$	49.6
11	1 wt% Nb_2O_5/α-Al_2O_3	$5.5 \cdot 10^{-1}$	39.7
13	SbO/SiO_2	$1.4 \cdot 10^{-2}$	43.3
14	Nb_2O_5	$3.2 \cdot 10^{1}$	61.0
20	NbPO	$1.2 \cdot 10^{2}$	66.1

3. References

1. G.C. Behera, K. Parida, Chem. Eng. J. 180 (2012) 270–276.
2. G.C. Behera, K. Parida, N.F. Dummer, G. Whiting, N. Sahu, A.F. Carley, M. Conte, G.J. Hutchings, J.K. Bartley, Catal. Sci. Technol. 3 (2013) 1558–1564.
3. F. Liu, H. He, Z. Lian, W. Shan, L. Xie, K. Asakura, W. Yang, H. Deng, J. Catal. 307 (2013) 340–351.
4. P.A. Kumar, Y.E. Jeong, H.P. Ha, Catal. Today 293–294 (2017) 61–72.
5. F. Berry, Hyperfine Interact. 111 (1998) 35–37.
6. J. Thrane, L.F. Lundegaard, P. Beato, U.V. Mentzel, M. Thorhauge, A.D. Jensen, M. Høj, Catalysts 10 (2020) 82.

7. K.V. Raun, L.F. Lundegaard, J. Chevallier, P. Beato, C.C. Appel, K. Nielsen, M. Thorhauge, A.D. Jensen, M. Høj, Catal. Sci. Technol. 8 (2018) 4626–4637.
8. M. Høj, T. Kessler, P. Beato, A.D. Jensen, J.D. Grunwaldt, Appl. Catal. A Gen. 472 (2014) 29–38.
9. M. Høj, A.D. Jensen, J.-D. Grunwaldt, Appl. Catal. A Gen. 451 (2013) 207–215.
10. V.N. Bibin, B.I. Popov, Kinet. Catal. 10 (1969) 1091–1098.
11. W.L. Holstein, C.J. Machiels, J. Catal. 162 (1996) 118–124.
12. A.M. Davies, S.H. Taylor, in: 236th Natl. Meet. Expo., American Chemical Society, Philadelphia, 2008.
13. A.M. Davies, Selective Oxidation and Oxidative Dehydrogenation Reactions Using Niobium Based Catalysts, Cardiff University, 2009.
14. H. Zhang, Z. Liu, Z. Feng, C. Li, J. Catal. 260 (2008) 295–304.
15. G.T. Whiting, J.K. Bartley, N.F. Dummer, G.J. Hutchings, S.H. Taylor, Appl. Catal. A Gen. 485 (2014) 51–57.
16. R. Häggblad, J.B. Wagner, S. Hansen, A. Andersson, J. Catal. 258 (2008) 345–355.
17. R. Häggblad, S. Hansen, L.R. Wallenberg, A. Andersson, J. Catal. 276 (2010) 24–37.
18. M. Massa, R. Häggblad, A. Andersson, Top. Catal. 54 (2011) 685–697.
19. A. Andersson, J. Holmberg, R. Häggblad, Top. Catal. 59 (2016) 1589–1599.
20. X. Wang, I.E. Wachs, Catal. Today 96 (2004) 211–222.
21. M. Thorhauge, (2017).
22. S.A. El-Molla, H.R. Mahmoud, Mater. Res. Bull. 48 (2013) 4105–4111.
23. N. Abadzhieva, D.G. Klisurski, Kinet. i Katal. 28 (1987) 735–736.
24. Y.L. Xiong, R. Castillo, C. Papadopoulou, L. Daza, J. Ladrière, P. Ruiz, B. Delmon, Stud. Surf. Sci. Catal. 68 (1991) 425–432.
25. I.E. Wachs, Catal. Today 27 (1996) 437–455.
26. Y. Chen, I.E. Wachs, J. Catal. 217 (2003) 468–477.